ELSEVIER

PII: S0032-3861(97)10259-2

Polymer Vol. 39 No. 21, pp. 5277–5280, 1998
0032-3861/98/$ – see front matter

Phase separation in a commercial block propylene–ethylene copolymer

Y. Feng and J. N. Hay*
School of Metallurgy and Materials, The University of Birmingham, Edgbaston, Birmingham B15 2TT, U.K.
(Revised 1 November 1997)

Phase separation in a commercial block propylene–ethylene copolymer has been studied by scanning electron microscopy (SEM). It was found that the size of the discrete domains within the copolymer increased with storage time in the melt. The particle coarsening had little or no effect on the crystallisation behaviour of the copolymers. The coarsening mechanism is that of Ostwald ripening. © 1998 Elsevier Science Ltd. All rights reserved.

(Keywords: block propylene–ethylene copolymer; phase separation; phase coarsening)

Introduction

At low temperature isotactic polypropylene is intrinsically brittle and suffers from poor fracture toughness. Improved impact strength have been obtained by copolymerisation with ethylene. The copolymerisation consists of modifying the standard propylene polymerisation process by adding a second monomer, usually ethylene, during the final stages of polymerisation. The morphology of such block copolymers are somewhat complex but the copolymer components form a phase separated system. The EPR is present as a minor fraction and the multiphase system is composed of a continuous matrix of PP with discrete particles of EPR.

PP is not compatible with EPR. Previous studies have addressed the evolution of a bicontinuous two-phase structure during spinodal decomposition, as reviewed recently by Hashimoto[1]. Phase separation may also occur by nucleation and growth of the dispersed domains. After the development of microstructure, the two-phase system will continue to evolve in response to its tendency to reduce the surface energy associated with interfacial area. This process, called coarsening, often results in a reduction in the number of droplets and an increase in their size.

Three different mechanisms have been described as being responsible for coarsening in the later stages of phase separation: Ostwald ripening, coalescence, and the hydrodynamic flow mechanism. In the first, Ostwald ripening, the total energy of the two-phase system composed of a dispersed second phase in a matrix decreases by an increase in the size of the second phase and thus a decrease in the total interfacial area. The classical theory of Ostwald ripening (the LSW theory was significantly developed by Lifshitz and Slyozov[2] and Wagner[3] by examining the case of widely spaced domains of a second phase growing and shrinking in a matrix. The diameter of the domains approximate to an asymptotic power-law growth behaviour[4]:

$$d = (D\xi)^{1/3} t^{1/3} \quad (1)$$

where d is the average domain size, D is a diffusion constant, ξ is the correlation length of the molecules, and t is the coarsening time.

In the coalescence mechanism, coarsening occurs by two or more droplets impinging on each other by translational diffusion to form a single droplet. Binder and Stauffer[5] explained the growth of clusters by simple molecular exchange as well as binary fission and fusion of droplets. The coalescence mechanism is also diffusion controlled and has a fractional power dependence on time[6]:

$$d = (k_B T/\eta)^{1/3} t^{1/3} \quad (2)$$

where k_B is the Boltzmann constant, T is temperature and η is the bulk viscosity. The same power dependence, $d \propto t^{1/3}$, holds for both Ostwald ripening and the coalescence mechanisms.

The third mechanism of coarsening is that of hydrodynamic flow[4,7]. According to Siggia[5], in the cylindrical part of the bicontinuous structure, the gradient of pressure along an axis of the cylinder causes a flow of the inner fluid from a narrow to a wide region, which results in coarsening of domains. In this mechanism, the growth rate is linear in time:

$$d = (\sigma/\eta)t \quad (3)$$

where σ is the surface tension. The basis for the hydrodynamic flow mechanism is that of an interfacial instability, phases of different size, and therefore different radii of curvature, have different pressures, which in turn cause flow[8].

More recently, Furukawa[9] formulated an asymptotic scaling function, indicating that there was only one length scale in the phase-separation system, and physical quantities depend on time only through this length scale. The scaling law is a more general form of the coarsening theory and the asymptotic behaviour of the characteristic length is depicted by

$$d = f(t^a) \quad (4)$$

with the exponent a depending on the microscopic mechanism of particle growth. The scaling hypothesis is consistent with the results of a numerical simulation using a kinetic Ising model[10]. Hashimoto *et al.*[11] and Bates and Wiltzius[12] have demonstrated in the case of polymer blends that a depends on time over a broad time scale, with a crossover between coarsening processes which is consistent with the idea put forth by Siggia[4].

Experimental

Materials. The block propylene–ethylene copolymer used in this work was supplied by SOLVAY, the grade number is

* To whom all correspondence should be addressed

RV210. It contained about 8 mol% ethylene overall. Fifteen percent by weight was amorphous EPR, about 30% was ethylene/propylene block copolymer with long ethylene and propylene sequences and the remainder polypropylene or copolymers with short ethylene sequences.

Polymer processing. A relatively homogeneous blend of the block copolymer was obtained by dissolving the resin in xylene at 130°C and precipitating at ambient temperature into methanol. This removed the amorphous EPR content. The material recovered was dried *in vacuo* and pressed at room temperature into opaque sheets. Quiescent melt ripening of these materials was carried out at low pressure on a hydraulic press heated to a specified melt temperature (e.g. 193°C) for specified periods of time, after which the samples were either quenched in ice water or slow cool to ambient temperature in air on a bench top.

SEM and stereology analysis. The ripened specimens were etched in *n*-heptane at 70°C for 30 min, and analysed in a JEOL 6300 SEM. The SEM photomicrographs were analysed with an image analyser—the particle areas being directly measured. The areas were assumed to be circular and the corresponding diameters were assumed to be the chord length of the particle. The required "true" particle diameter distribution moments (d_n, d_w and d_z) were calculated from the chord lengths according to previously published statistical analysis methods of stereology[12]. The chord lengths obtained were converted to diameters of the three-dimensional structure with the following procedure and stereological formulae:

(1) In collecting the (l_i, N_i) data, where l_i is the chord length and N_i: the number of chords;

(2) To calculate chord length averages:

$$\text{Harmonic average}: \bar{l}_H = \sum N_i / \sum \frac{N_i}{l_i} \quad (5)$$

$$\text{Number average}: \bar{l}_n = \frac{\sum N_i l_i}{\sum N_i} \quad (6)$$

$$\text{Weight average}: \bar{l}_w = \frac{\sum N_i l_i^2}{\sum N_i l_i} \quad (7)$$

(3) To calculate particle diameter averages:

$$\text{Number average}: \bar{d}_n = \bar{l}_H\left(\frac{\pi}{2}\right) \quad (8)$$

$$\text{Weight average}: \bar{d}_w = \bar{l}_n\left(\frac{4}{\pi}\right) \quad (9)$$

$$Z-\text{average}: \bar{d}_z = \bar{l}_w\left(\frac{3\pi}{8}\right) \quad (10)$$

$$\text{Polydispersity}: PD = \frac{\bar{d}_w}{\bar{d}_n} \quad (11)$$

Results and discussion

The SEM photomicrographs of the coarsening of the domains in the ice water-quenched and slow-cooled samples are shown in *Figure 1*. The particles grew larger with storage time left in the melt and correspondingly the

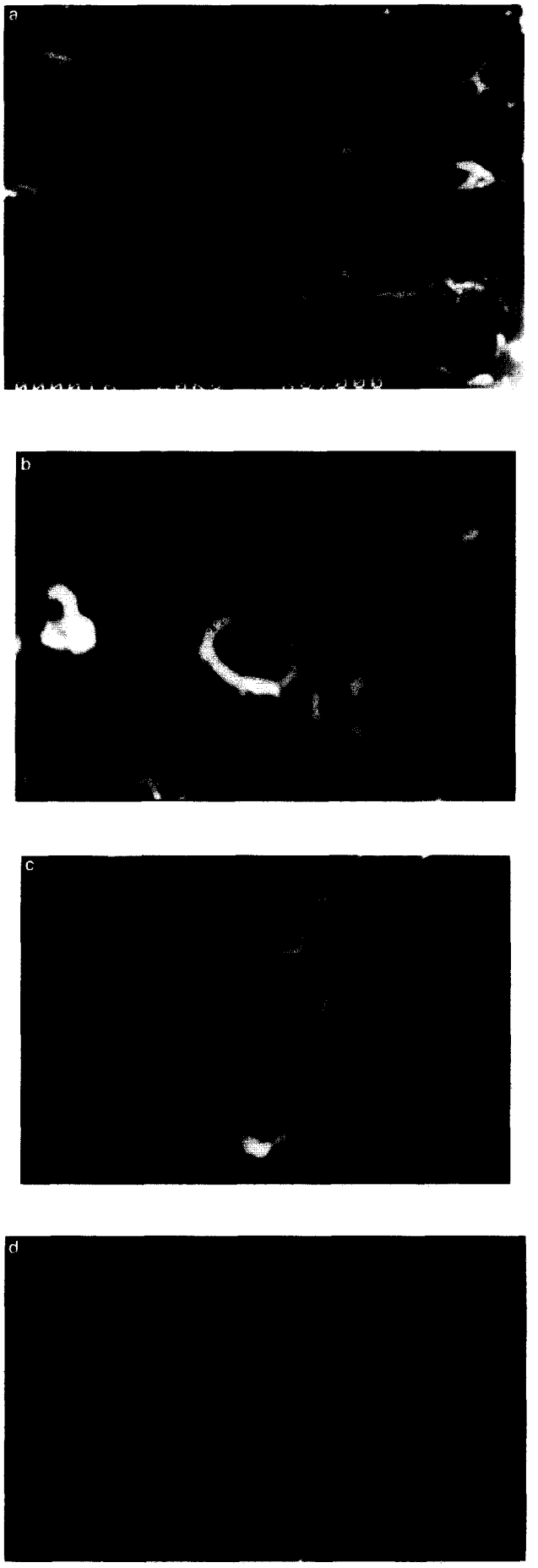

Figure 1 SEM photomicrographs. Ice quenched specimen (a) initially and (b) after storage for 480 s in the melt. Slow cooled specimen (c) initially and (d) after storage for 900 s in the melt

Table 1 Particle diameter distributions for the ice water-quenched samples

Coarsening time (s)	d_n (μm)	d_w (μm)	d_z (μm)	d_w/d_n ±0.2	d_z/d_w ±0.2	Number of particles (mm^{-2})
5	0.28	0.28	0.36	1.3	1.0	185 ± 10
45	0.55	0.58	0.66	1.2	1.1	170
120	0.66	0.80	1.17	1.2	1.5	55
480	0.71	0.78	0.79	1.1	1.0	56
3600	1.11	1.15	1.35	1.0	1.2	54

Table 2 Particle diameter distributions for the slow cooled samples

Coarsening time (s)	d_n (μm)	d_w (μm)	d_z (μm)	d_w/d_n ±0.2	d_z/d_w ±0.2	Number of particles (mm^{-2})
45	0.31	0.31	0.41	1.0	1.3	225 ± 25
480	0.38	0.38	0.44	1.0	1.2	127
900	0.37	0.43	0.47	1.1	1.2	152
3600	0.68	0.73	0.89	1.1	1.2	63

number of particles per unit area decreased. Particle diameter distributions were determined by measuring a representative population of the particle areas and then applying stereological methods[13]. *Figure 2a* shows the particle diameter distribution for the ice water-quenched samples. It can be seen that the distributions are not regular, but with increasing coarsening time, the distribution curve shifted to larger diameters. For slow-cooled samples, the same phenomenon was observed, see *Figure 2b*. At the same time, the particle size distribution, initially quite narrow, tended to broaden at longer coarsening time. The particle diameter averages are presented in *Table 1* and *Table 2* for the ice water-quenched samples and slow cooled samples, respectively.

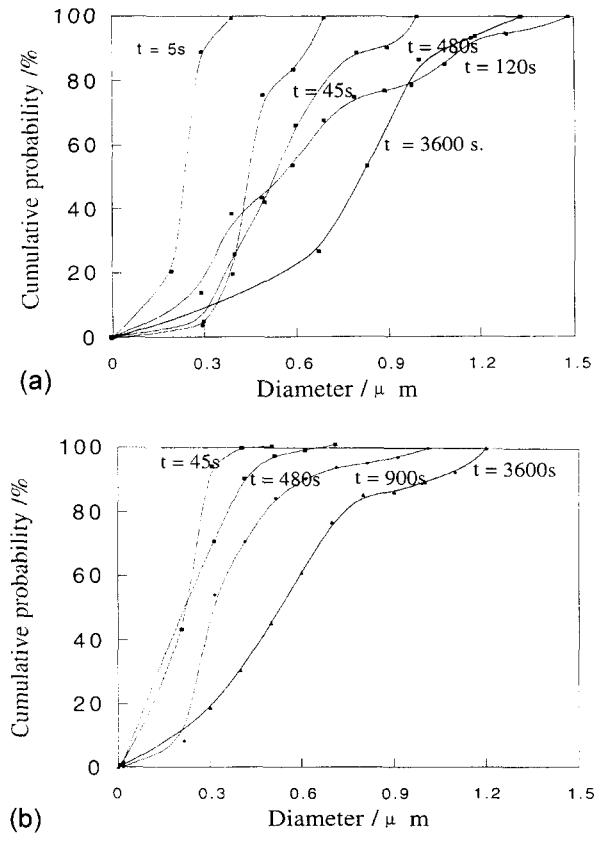

Figure 2 Particle diameter distribution (± 2.5%) after various storage times in the melt, (a) ice-water quenched and (b) slow cooled samples

The coarsening of the ice water-quenched samples was measured and plotted as d_w^3 versus time t in *Figure 3*. It can be seen that the coarsening process can be divided into a short and a long-time regime. Little is known about the nucleation and growth process and the particle size distribution that is produced in the short-time regime[14]. Furthermore, the shift from the short-time regime to the asymptotic long-time regime, and its effect on particle size distribution has been little studied[14]. However, for the long-time regime, the $d_w^3 \sim t$ relationship is linear, in accordance with equations (1) and (2), the slope giving the coarsening constant.

The coarsening data for the bench slow cooled samples are also plotted in *Figure 3*. It can be seen that the data follow approximately the same trend of d_w growth with $t^{1/3}$, as observed for the ice water-quenched samples. It can say that the different modes of crystallisation had little or no effect on the particle coarsening process.

The number of particles per unit area N_A is related to the particles per unit volume as follows [13]:

$$N_A = Nd_n \tag{12}$$

According to the prediction,

$$N \sim t^{-1} \tag{13}$$

For both ice water-quenched samples and air quenched samples, see *Figure 4*, the $N \sim t^{-1}$ behaviour is not approached until long times.

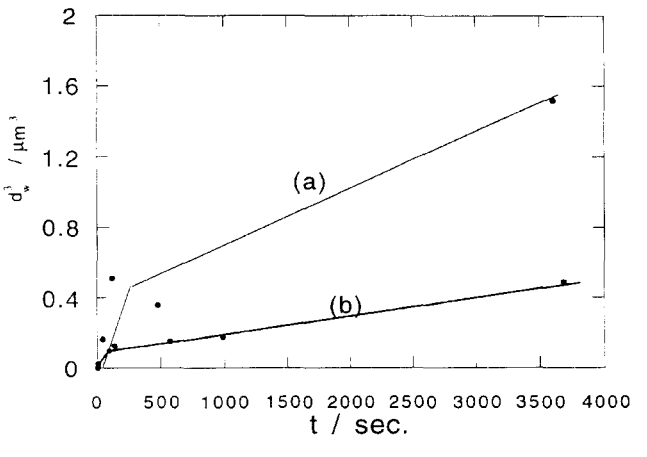

Figure 3 Variation of particle diameter, d_w^3 with coarsening time t. (a) ice water quenched and (b) slow cooled samples

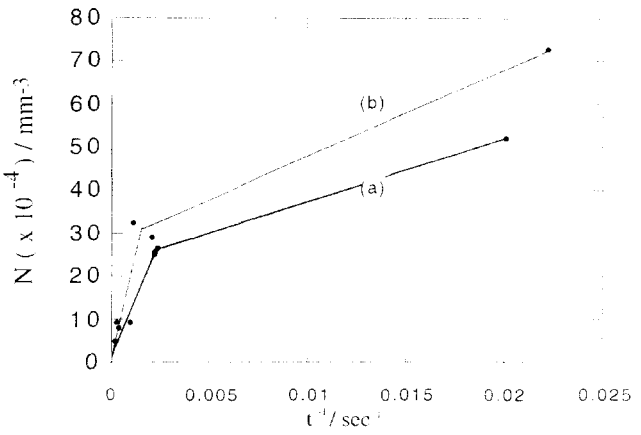

Figure 4 Variation of number of particles, N, with reciprocal coarsening time t. (a) ice water quenched and (b) slow cooled samples

The above results are in agreement with both the Ostwald ripening and the Coalescence mechanisms. However, for both samples, the coarsening rate constant K was found to be about 10^{-4} $\mu m^3 s^{-1}$. This value is closer to the Ostwald ripening rate constant: K_{or}, said to be 10^{-4}–10^{-6} [15], and coalescence would then be negligible.

Conclusions

A two-phase morphology of block propylene-ethylene copolymer was generated in the melt state. Small nuclei of particles appeared at short time and increased in volume with increasing time in the melt state. The coarsening of the minor phase EPR component in the bulk propylene–ethylene copolymer has been shown to follow the theoretically predicted $d \sim t^{1/3}$ and $N \sim t^{-1}$ (where d = diameter, N = number of particles, and t = time in melt) relationships to a close approximation. At short times these relationships were not obeyed. The indication was that the long-time coarsening regime was not entered until several minutes elapsed in the melt state. The particle size distribution was initially quite narrow and exhibits a trend of broadening at longer times of coarsening. This may be due to the shift from the short-time regime to the longer-time coarsening regime. The coarsening mechanism is suggested to be Ostwald ripening.

Acknowledgements

Y. Feng is pleased to acknowledge the award of a research grant from Sino-British Friendship Scholarship Scheme (SBFSS) during the tenure of this work.

References

1. Hashomoto, T., *Phase Transitions*, 1988, **12**, 47.
2. Lifshitz, I. M. and Slyozov, V. V., *J. Phys. Chem. Solids*, 1961, **19**, 35.
3. Wagner, C., *Z. Elektrochem.*, 1961, **65**, 581.
4. Siggia, E. D., *Phys. Rev. A.*, 1979, **20**, 595.
5. Binder, K. and Stauffer, D., *Phys. Rev. Lett.*, 1974, **33**, 1006.
6. Chou, Y. C. and Goldburg, W. I., *Phys. Rev. A.*, 1979, **20**, 2105.
7. Voigt-Martin, I. G., Leister, K. H., Rosenaic, R. and Koningsveld, R., *J. Polym. Sci. (Phys.)*, 1986, **24**, 723.
8. Aubert, J. H., *Macromolecules*, 1990, **23**, 1446.
9. Furukana, H., *Adv. Phys.*, 1985, **34**, 703.
10. Marro, J., Lebowits, J. L. and Kalos, M. H., *Phys. Rev. Lett.*, 1979, **43**, 282.
11. Hashimoto, T., Itakura, M. and Hasegawa, H., *J. Chem. Phys.*, 1986, **85**, 6118.
12. Bates, F. S. and Wiltzius, P., *J. Chem. Phys.*, 1989, **91**, 3258.
13. Weibel, E. R., *Stereological Methods*, Vol. 2, *Theoretical Foundations*. Academic Press, London, 1980.
14. Voorhees, P. W., *J. Stat. Phys.*, 1985, **38**, 231.
15. Mirabella, F. M. and Barley, J. S., *J. Polym. Sci. (Phys.)*, 1994, **32**, 2187.